**Cell Reports, Volume *36***

## Supplemental information

# A molecular sensor determines the ubiquitin substrate specificity of SARS-CoV-2 papain-like protease

**Stephanie Patchett, Zongyang Lv, Wioletta Rut, Miklos Békés, Marcin Drag, Shaun K. Olsen, and Tony T. Huang**

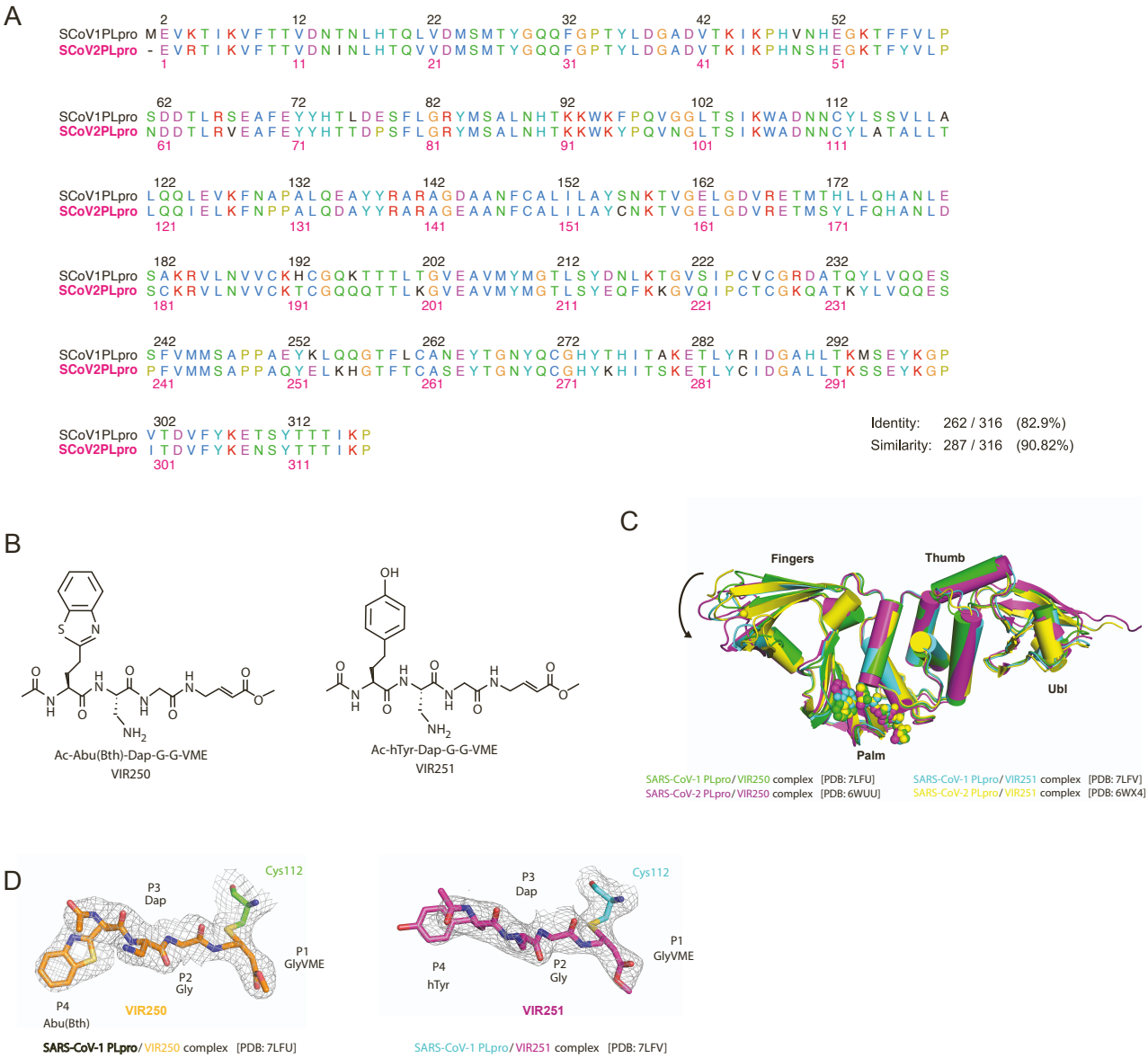


**Figure S1. PLpro alignments and inhibitor schematics, Related to Figure 1. A)** Schematic of VIR250 and VIR251 inhibitors. **B)** Crystal structures of SCoV-1 and SCoV-2 PLpro with VIR250 and VIR251 aligned. VIR250 and VIR251 shown as spheres, arrow highlights slight rotation of the fingers domain. **C)** Sequence alignment of PLpro domain from SARS-CoV-1 and SARS-CoV-2, aligned using Local alignment (Smith-Waterman). SCoV-1 PLpro amino acid numbering is shown above the alignment (black) and SCoV-2 numbering is shown below the alignment (magenta). **D)** 2FoFc electron density maps of VIR250 (left) and VIR251 (right) contoured at 1.0σ and shown as mesh.

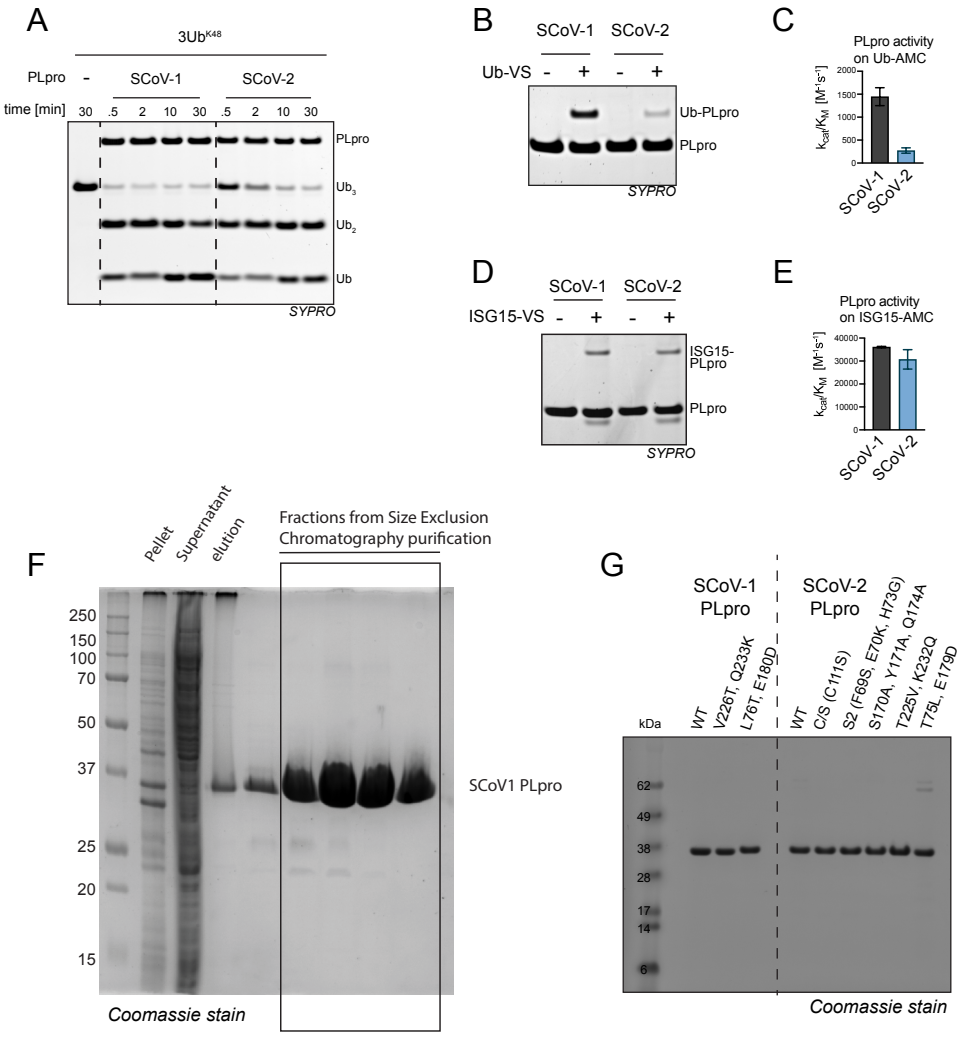


**Figure S2. Comparison of SCoV-1 and SCoV-2 PLpro activity, Related to Figures 2, 3 and STAR Methods. A)** Cleavage of K48-linked tetra-Ub chains (3UbK48) by SARS-CoV-1 vs. SARS-CoV-2 PLpro. **B)** Ub-Vinyl Sulfone (Ub-VS) labeling of SARS-CoV-1 vs. SARS-CoV-2 PLpro. **C)** Relative apparent kcat/KM values for hydrolysis of Ub-AMC by SARS-CoV-1 and SARS-CoV-2 PLpro. **D)** ISG15-VS labeling of SARS-CoV-1 vs. SARS-CoV-2 PLpro. Experiments in **A, B, D** were repeated at least three times with similar results. **E)** Relative apparent kcat/KM values for hydrolysis of ISG15-AMC by SARS-CoV-1 and SARS-CoV-2 PLpro. Error bars in **C, E** represent SD (n = 3 independent experiments). **F)** Last step of SCoV-1 PLpro purification on size exclusion chromatography, analyzed by SDS-PAGE and Coomassie staining. The pure fractions were pooled and concentrated. **G)** Purified SCoV-1 and SCoV-2 PLpro and mutants (2 μM) analyzed by SDS-PAGE and Coomassie staining.

**Table S1. Crystallographic Data and Refinement Statistics, Related to Figure 1.**

| | SARS-CoV-1 PLpro/VIR250 complex | SARS-CoV-1 PLpro/VIR251 complex |
|---|---|---|
| PDB ID | 7LFU | 7LFV |
| Source | APS 24 IDE | APS 24 IDE |
| Wavelength (Å) | 1.00 | 1.00 |
| Resolution Limits (Å) | 70.7-2.29 (2.37-2.29) | 132.7-2.23 (2.30-2.23) |
| Space Group | I222 | $P6_122$ |
| Unit Cell (Å) *a*, *b*, *c* | 70.8, 90.4, 113.6 | 103.6, 103.6, 265.4 |
| Unit Cell (°) $\alpha$, $\beta$, $\gamma$ | 90, 90, 90 | 90, 90, 120 |
| Number of observations | 108176 | 1632487 |
| Number of reflections | 16767 (1626) | 42208 (3796) |
| Completeness (%) | 100 (100) | 99.9 (99.3) |
| Mean I/$\sigma$I | 16.0 (0.7) | 30.9 (2.0) |
| $CC_{1/2}$ | 0.9986 (0.408) | 1.00 (0.756) |
| $R_{merge}$ [a] | 0.074 (2.15) | 0.099 (2.04) |
| $R_{pim}$ | 0.032 (0.962) | 0.016 (0.341) |
| | | |
| <u>Refinement Statistics</u> | | |
| Resolution Limits (Å) | 70.7-2.29 (2.36-2.29) | 53.3-2.23 (2.28-2.23) |
| # of reflections (work/free) | 16663 (1668) | 42096 (2000) |
| Completeness (%) | 99.3 (93.0) | 99.9 (99.0) |
| Protein/solvent/ligand atoms | 2414/0/36 | 5009/156/35 |
| $R_{cryst}$ [b] | 0.224 (0.360) | 0.197 (0.297) |
| $R_{free}$ | 0.265 (0.380) | 0.235 (0.352) |
| Bonds (Å)/ Angles (°) | 0.003/0.499 | 0.009/1.078 |
| B-factors: protein/solvent/ligand (Å$^2$) | 91.5/--/84.2 | 64.8/62.9/79.4 |
| Ramachandran plot statistics (%) | | |
| favored | 96.3 | 96.8 |
| allowed | 3.7 | 3.2 |
| outliers | 0 | 0 |
| MolProbity score | 1.81- 96$^{th}$ percentile (N=8848, 2.29 Å ± 0.25Å) | 1.64- 97$^{th}$ percentile (N=10112, 2.23 Å ± 0.25Å) |

Parentheses indicate statistics for the high-resolution data bin for x-ray data.
a. $R_{merge} = \sum hkl \sum i|I(hkl)i - \langle I(hkl)\rangle|/\sum hkl\sum i \langle I(hkl)i\rangle$.
b. $R_{cryst} = \sum hkl\ |Fo(hkl)-Fc(hkl)|/\sum hkl\ |Fo(hkl)|$, where *Fo* and *Fc* are observed and calculated structure factors, respectively.